The Role of Land Surface Schemes in Short-Range, High Spatial Resolution Forecasts

LEI WEN AND WEI YU

Centre de recherche en calcul appliqué, Montreal, Quebec, Canada

CHARLES A. LIN

Centre de recherche en calcul appliqué, and Department of Atmospheric and Oceanic Sciences and Centre for Climate and Global Change Research, McGill University, Montreal, Quebec, Canada

MICHEL BELAND

Centre de recherche en calcul appliqué, Montreal, Quebec, Canada

ROBERT BENOIT AND YVES DELAGE

Recherche en prévision numérique, Atmospheric Environment Service, Environment Canada, Montreal, Quebec, Canada

(Manuscript received 26 July 1999, in final form 28 February 2000)

ABSTRACT

Many studies have demonstrated the importance of land surface schemes in climate change studies using general circulation models (GCMs). However, there have not been many studies that explore the role of land surface schemes in the context of short-range and high spatial resolution precipitation forecasts. The motivation of this study is to examine the sensitivity of simulated precipitation, and sensible and latent heat fluxes, to the use of different land surface schemes at two different spatial resolutions. The meteorological model used is the Mesoscale Compressible Community (MC2) model, and the land surface schemes are the force–restore method and the Canadian Land Surface Scheme (CLASS). Parallel runs have been performed using MC2/CLASS and MC2/force–restore at spatial resolutions of 10 and 5 km to simulate the severe precipitation case of 19–21 July 1996 in the Saguenay region of Québec, Canada. Comparisons of the simulated precipitation time series and the simulated 48-h accumulated precipitation at different spatial resolutions with rain gauges indicate that MC2/CLASS at 5-km resolution gives the best simulated precipitation. The comparison results show the model accuracy of MC2/CLASS at 10 km is comparable to the accuracy of MC2/force–restore at 5 km. The mechanism responsible for this is that CLASS represents the land surface vegetation characteristics in a more sophisticated manner than the force–restore method. Furthermore, in CLASS, each grid square is divided into a maximum of four separate subareas, and subvariations of the grid surface vegetation characteristics are taken into account. Therefore, for a grid square containing different types of vegetation, the subgrid-scale information can be used by CLASS, and the computed effective variables that are fed back to MC2 on a 10×10 km^2 grid are equivalent to computing them at a higher effective resolution than 10 km. This higher effective resolution for surface characteristics is not found in the force–restore method. The total simulated domain-averaged precipitation, and the sum of sensible and latent heat fluxes from MC2/CLASS and MC2/force–restore at different spatial resolutions, are similar. The major difference is in the partitioning of the simulated sensible and latent heat fluxes. The positioning of the simulated precipitation has been improved by using CLASS. The overall results suggest that the impact of land surface schemes is indeed significant in a short-range precipitation forecast, especially in regions with complicated vegetation variations.

1. Introduction

Observed occurrence of severe flood events has risen over recent years. To minimize the effect of severe flood damages, the establishment of an accurate and timely flood warning system (FWS) is of prime importance. Obtaining accurate and timely precipitation data is a central concern associated with the full implementation of a hydrological model within an FWS. Coupling to a well-established, high-resolution numerical weather forecast model not only offers a valid alternative to avoid possible problems linked with acquiring good precipitation data, but also provides a means for extending

Corresponding author address: Dr. Lei Wen, Centre de recherche en calcul appliqué, 5160 Boul. décarie, bureau 400, Montréal, PQ H3X 2H9, Canada.
E-mail: leiwen@cerca.umontreal.ca

the flood forecast period. A complete two-way coupled hydrometeorological modeling system uses a land surface scheme as the common interface between the meteorological and hydrological components.

Over the past three decades numerous land surface schemes have been developed, implemented, and tested for various climate conditions around the world. These land surface schemes vary in complexity from the very simple bucket method (Manabe 1969; Deardorff 1978) to more physically based schemes (e.g., Sellers et al. 1986, 1996; Noilhan and Planton 1989; Verseghy 1991; Verseghy et al. 1993; Yang and Dickinson 1996). In the Project for Intercomparison of Land-surface Parameterization Schemes, several studies have reported on and discussed the performances of some well-known land surface schemes (Henderson-Sellers et al. 1993; Yang et al. 1995; Shao and Henderson-Sellers 1996; Chen et al. 1997). Although most land surface schemes have been validated and calibrated with the help of field data, the differences between individual models may still be large. Despite the fact that considerable work is still needed to examine the physical basis of existing surface–vegetation–atmosphere transfer schemes, as well as to identify the techniques leading to the best modeling results, the physically based land surface schemes have the most promising potential for meteorological, hydrological, and agricultural applications (Wen et al. 1998).

Numerous investigations have demonstrated the importance of land surface schemes in climate change studies using general circulation models (GCMs) (e.g., Rowntree and Bolton 1983; Bouttier et al. 1993; Nobre et al. 1991; Garratt 1993; Milly and Dunne 1994; Noihan and Lacarrère 1995; Rosenzeig and Abramopoulos 1997). However, there have been few studies that explore the role of land surface schemes in the context of short-range and high spatial resolution precipitation forecasts. Aside from the limitation of computing power, one may posit that land surface schemes may not be important for short-range precipitation forecasts, since the atmosphere may not have enough time to react to any significant energy flux changes occurring at the surface within a short period of time. In this study, we examine the accuracy of this hypothesis.

The sensitivity of numerically simulated climates to land surface boundary conditions has been studied by Mintz (1984), who concluded that a coupling exists between evaporation and precipitation in the sense that precipitation increases over land as evaporation increases. In this case a positive feedback from the recirculation of precipitation should be expected through the soil moisture reservoir. Using GCMs, a similar result was found by Oglesby (1991) and Beljaars et al. (1996) from short- and medium-range model simulations. Although the precipitation response to evaporation is marked, just how this response works in detail at high spatial resolution is still unknown. Furthermore, as mentioned previously, differences between individual land surface schemes can be large. It is not clear how these differences will manifest themselves in three-dimensional (3D) precipitation simulation, particularly at high spatial resolution. Therefore there is a practical need to examine the role of land surface schemes in the context of short-range and high spatial resolution precipitation forecasts.

For this study, the meteorological model used is the Mesoscale Compressible Community (MC2) model. The land surface schemes are the force–restore method and the Canadian Land Surface Scheme (CLASS). To determine the impact of land surface schemes on short-range, high spatial resolution precipitation forecasts, we examine the severe precipitation case of 19–21 July 1996 in the Saguenay region of Québec, Canada, which led to severe flooding. A series of 48-h simulations with spatial resolutions of 10 and 5 km have been performed using the MC2/CLASS and the MC2/force–restore modeling systems. The precipitation results are compared with observations from surface stations. In order to gain further insight into the mechanisms responsible for the difference in precipitation forecasts, three more MC2/CLASS runs at 10 km with uniform coniferous trees, grass, and bare soil were performed. We also examine the sensitivities of simulated domain-averaged precipitation, and sensible and latent heat fluxes to the use of two different land surface schemes (force–restore method and CLASS) at different spatial resolutions. The simulated surface flux distribution and the resulting precipitation distribution are analyzed. The results suggest that the impact of land surface schemes can be significant in a short-range precipitation forecast, especially in regions with complicated vegetation variations.

2. MC2/CLASS and MC2/force–restore modeling systems

MC2 is a limited-area 3D atmospheric research model developed over the last seven years at Recherche en prévision numérique (RPN), Environment Canada. The motivation of the development of MC2 is to provide a versatile modeling tool to meet a variety of needs of the atmospheric research community in Canada at a fine spatial scale. A land surface scheme must be incorporated into MC2 to provide lower boundary conditions. The force–restore method is a simple but widely used land surface scheme that currently serves as the operational model at the Canadian Meteorological Centre (CMC). It is a perfectly valid method for formulating land surface equations. The importance of the use of physically based land surface schemes has been described in the previous section. CLASS is such a physically based land surface model developed at Environment Canada's Climate Research Branch, which has been incorporated into the unified RPN physics package. CLASS has been tested and validated in both standalone and coupled modes with the Canadian General Circulation Model and Canadian global forecast model under different soil types, in addition to different land coverage and meteorological conditions (Wen et al.

TABLE 1. Summary of MC2, force–restore, and CLASS models.

MC2 model
Dynamics
3D, fully elastic, nonhydrostatic Navier–Stokes equations in Tanguay et al. (1990)
Semi-Lagrangian advection and semi-implicit time differencing scheme
Gal-Chen and Sommerville (1975) vertical coordinate
Staggered vertical and horizontal grids (Arakawa C grid)
One-way nesting technique for the lateral and upper boundary conditions
Physics
Planetary boundary layer based on turbulent kinetic energy
Fully implicit vertical diffusion
Stratified surface layer based on similarity theory
Diurnal cycle with solar and infrared fluxes at ground modulated by diagnostic clouds
Solar and infrared radiation schemes fully interactive with clouds
Shallow convection parameterization
Sundqvist parameterization for resolved-scale condensation (Sundqvist 1978; Yu et al. 1998) and Kuo's parameterization for subgrid-scale convection (Kuo 1974)
Force–restore model
Two soil layers for temperature for each grid cell
Diffusion-based solution for the heat balance and fixed moisture treatment
A simple snowmelting scheme of the RPN physics package
CLASS model
Three prognostic soil layers for each grid cell, assuming both soil heat flux and water suction gradient are zero at the bottom of the third layer
In soil, heat is transferred by conduction while moisture flux follows Darcy's law
At the surface, each grid cell can be divided into as many as four subareas: bare soil, canopy covered, snow covered and snow and canopy covered
Taken into account up to four vegetation canopies: needleleaf forest, broadleaf forest, crops, and grasses
α or β bare soil evaporation model of Wen et al. (1998)

TABLE 2. Force–restore and CLASS main inputs and outputs.

Force–restore model	CLASS model
Inputs	Inputs
Vegetation index (V_G)	Vegetation coverage (f_r)
Surface albedo (A_l)	Leaf area index (LAI)
Roughness length (z_p)	Vegetation roughness (z_0)
Launching height (L_H)	Visible albedo (α_{VIS})
Soil moisture content index (H_S)	Near-infrared albedo (α_{NIR})
Deep soil temperature (T_p)	Canopy mass (W_C)
	Rooting depth (z_r)
	Clapp and Hornberger (1978) soil empirical parameter (b)
	Saturated soil moisture content (θ_p)
	Saturated soil suction (ψ_{sat})
	Saturated hydraulic conductivity (k_{sat})
	Soil color
	Soil drainage
Outputs	Outputs
Surface temperature (T_S)	Canopy temperature (T_C)
Sensible heat flux (F_C)	Depth-averaged soil temperatures (T_B) for three layers
Latent heat flux (F_V)	Depth-averaged soil moisture content (θ_B) for three layers
	Sensible heat flux (F_C)
	Latent heat flux (F_V)

1998; Delage and Verseghy 1995; Verseghy 1991; Verseghy et al. 1993). Detailed descriptions of MC2, the force–restore method, and CLASS can be found in Benoit et al. (1997), Manabe (1969), Deardorff (1978), Verseghy (1991), and Verseghy et al. (1993). The principal characteristics of MC2, the force–restore method, and CLASS are summarized in Table 1. The force–restore method and CLASS soil and vegetation input parameters and simulated outputs are listed in Table 2. Note that all temperature and soil moisture content variables in the output list must be initialized at the beginning of the integration.

Perhaps the most important feature of MC2 is that it is one of the few currently available 3D, fully elastic, nonhydrostatic models that uses semi-Lagrangian advection with a semi-implicit time-differencing scheme (SLSI). It is mainly due to the use of the SLSI technique that MC2 has become one of the world's most efficient models in facilitating simulations over a wide spectrum of spatial scales (varying from 2 to 200 km). Recently, a new generalized minimal residual Krylov iterative solver and a more efficient semi-Lagrangian advection scheme have been included in MC2 (Thomas et al. 1998).

The force–restore method is used in many GCMs and atmospheric models for the specification of land surface conditions. It is a closure condition on the heat and moisture balances at the air–soil interface, with unknown subsurface ground fluxes modeled as diffusive processes. Modifications to the force–restore method have been introduced recently at RPN (Mailhot et al. 1997) to include 1) an improved calculation of land surface evaporation and evapotranspiration, 2) a more sophisticated snow and ice representation, and 3) a better modeling of snowmelt in the surface energy balance.

CLASS is a physically based 1D column model that has been designed to represent the average characteristics of a horizontal grid square. Each grid square is divided into a maximum of four separate subareas, respectively distinguished by 1) bare soil, 2) snow cover (alone), 3) vegetation cover (alone), and 4) both snow and vegetation cover. In the case of bare soil, the absorption of solar radiation is modeled to be a function of soil color and wetness, and atmospheric resistance taken to follow Monin–Obukhov's similarity theory. Precipitation is then treated in one of the following three ways: as infiltration to the soil, as retention on the surface, or as drainage (runoff). The snow subarea introduces an extra layer of variable thickness on top of the soil. The last two subareas containing vegetation (marked by presence and absence of snow) are themselves composed of four types of vegetation: needleleaf

trees, broadleaf trees, crops, and grasses. This accounts for variations of surface vegetation characteristics. The composite vegetation layer of CLASS includes a physically based but separate treatment of energy and moisture fluxes from the layer, in addition to radiation and precipitation falling through it, while also incorporating an explicit thermal separation of the vegetation underground. The ''mosaic'' approach is then used to calculate the effective surface fluxes over a grid cell. These averaged surface fluxes are obtained by averaging surface fluxes calculated over an ensemble of subarea land surface patches. The importance and advantages of the mosaic approach are discussed in Avissar and Pielke (1989), Koster and Suarez (1992), Wood et al. (1992), and Ducoudré et al. (1993). Each subarea shares the same soil variables. CLASS includes three soil layers, with physically based calculations of heat and moisture transfer at the surface and across the layer boundaries. The standard soil layer thicknesses are 0.10, 0.25, and 3.75 m down to 4.10 m from the surface. The depth-averaged temperature and moisture content are modeled for each of the three soil layers. In addition to the initialization of CLASS parameters, CLASS is driven by continuous total long- and shortwave radiation at the ground surface, as well as by the following fields provided by MC2: precipitation rate, air temperature, wind speed, specific humidity of the air, and atmospheric pressure near the ground surface. Two major feedback variables from the force–restore method and CLASS are sensible and latent heat fluxes (see Table 2).

In this study, the precipitation process in MC2 is modeled using the Sundqvist (1978) parameterization for resolved-scale condensation, with improvements in each of the following four areas: 1) the representation of coalescence, 2) the Bergeron–Findeinsen mechanism, 3) the cirrus mechanism (Yu et al. 1998), as well as 4) Kuo's (1974) scheme for parameterization of subgrid-scale convection. A number of improvements have been made since the official release of CLASS version 2.6. These include a new evaporation model over bare soil (Wen et al. 1998) and the use of the blending height method for averaging roughness length to replace the logarithmic average employed in the standard version of CLASS (Delage et al. 1999). The only difference in the MC2/CLASS and MC2/force–restore modeling systems is the use of the land surface schemes.

3. Model formulation for the Saguenay storm

As mentioned already, we have used both MC2/CLASS and MC2/force–restore modeling systems to examine a severe precipitation case in the Saguenay region of Québec, Canada, which led to a flash flood event during 19–21 July 1996.

Simulations have been performed on two horizontal grid configurations (10- and 5-km resolutions), on Environment Canada's NEC SX-4 supercomputers. All simulations started at 1200 UTC 19 July and ended at 1200 UTC 21 July 1996, with no spinup period. We compute differences in 48-h accumulated precipitation (PR48) between the model simulations and observations. We then analyze observed and simulated precipitation time series at different locations. In addition to the precipitation field, differences in the simulated sensible and latent heat fluxes due to the use of two land surface schemes at different spatial resolutions are also discussed. These differences reflect the impact of the two land surface schemes (force–restore method and CLASS).

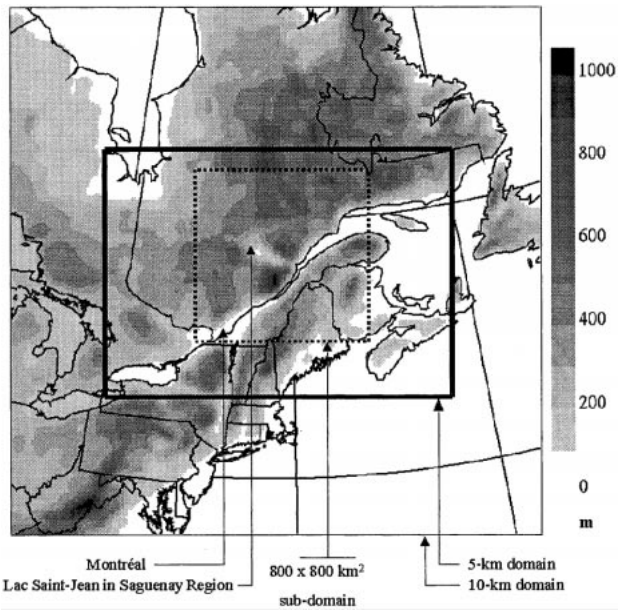

FIG. 1. Simulation domains for the two resolutions: 1) 331 × 231 grid points at 5 km, and 2) 251 × 251 grid points at 10 km. Both domains are centered at 48°N and 71°W. The dotted line shows the subdomain covering the Saguenay region and its immediate vicinity discussed in subsequent figures. The grayscale shows surface topography (m) at 10-km resolution.

a. The July 1996 Saguenay severe precipitation case

The Saguenay region is located to the northeast of Montréal, province of Québec, Canada (Fig. 1), with an area of approximately 10 000 km^2. The Saguenay River runs from the northwest to the southeast, from Lac Saint-Jean toward the tidewater at the head of the Saguenay Fjord that joins the St. Lawrence River. Two hills are located along the river valley, in the south (with a height of 1086 m) and the north (875 m). The region is underlain by granitic and gneissic rocks from the Grenville Province of the Canadian Shield. Glacial till and sparse fluvioglacial deposits form the mantle of this Cambrian bedrock area. The mixed forest (coniferous and deciduous trees) and closed coniferous forest (with accompanying patches of grasses) provide the dominant vegetation in the Saguenay region and its immediate vicinity, according to the Geographic Information Sys-

tem (GIS) database (1-km resolution) obtained from Environment Canada. This has been confirmed by our own two-day field and airborne survey in the summer of 1998.

During 19–21 July 1996, a record-breaking flash flood resulted from an unprecedented heavy rainfall in the Saguenay region. Synoptically, this severe precipitation event can be traced back to a small perturbation located over southern Manitoba, Canada, characterized by a central sea level pressure (SLP) of 1002 mb. This small low pressure system rapidly deepened as it moved northeastward beyond Lake Ontario starting 1200 UTC 19 July 1996. By the time it reached the eastern Saguenay region 24 h later, this low pressure system had deepened considerably in SLP, from 999 to 979 mb. Over the next day, it slowed and ultimately remained quasi-stationary over the Gaspé Peninsula of Québec (Yu et al. 1997). The low pressure system produced intense precipitation over 48 h, concentrated over the Saguenay region and extending eastward along the lower north shore of the Gulf of St. Lawrence. The average accumulated precipitation over the 48-h period was in excess of 200 mm over a 5000 km^2 area.

There were 46 Environment Canada and Environment Québec rain gauges distributed along the valley of the St. Lawrence River and in the Saguenay region that functioned during the storm. Each rain gauge record was visually inspected for discontinuities. Most of the rain gauges were concentrated around the mountainous area, south of the Saguenay River and the St. Lawrence River valley. The synoptic flow was from the north in the Saguenay region. The analysis of the rain gauge data indicated that there were two strong precipitation centers on the windward and upslope side of the mountainous regions. The observed maximum value of 48-h accumulated precipitation reported among these stations was 274.3 mm, which occurred on the windward side of a high plateau region, south of the Saguenay River. This value was approximately two to three times the largest previously recorded maximum going back over a period of 120 years. However, there were only a few rain gauges in the northern mountainous region, probably due to the fact that this region is less populated. As a result, the observed maximum PR48 of 183.8 mm in the northern mountainous region might be an underestimate of the true maximum. This hypothesis has been qualitatively confirmed with the infrared image from the Geostationary Operational Environmental Satellite (GOES), taken at 1745 UTC 20 July 1996. The timing of the image taken coincided with the occurrence of the second wave of heavy precipitation. The image clearly shows a lower brightness temperature and a higher cloud albedo over the northern compared to the southern mountainous region (Yu et al. 1997), thus indicative of deep clouds in the northern region. The model results will be shown in section 4.

In mountainous areas, the area representativeness of a rain gauge can be contaminated by many uncertain factors, such as the variation of altitude within a grid cell. This leads to uncertainty in the comparison of the simulated precipitation (which represents the average over a grid cell) and the observed value at the rain gauge location. This will also introduce many uncertainties in an effort to plot horizontal distribution of observed precipitation available only at a few rain gauges. It is difficult to quantify these uncertainties and this is still a subject attracting attention. The use of a high spatial resolution model may help to reduce the uncertainty relating to point-by-point comparison.

b. Model configuration and initialization

The Saguenay simulation experiments were done at two horizontal resolutions: 10 and 5 km (Fig. 1). The MC2/CLASS and MC2/force–restore modeling systems were configured on the same polar stereographic projection with $251 \times 251 \times 25$ and $331 \times 231 \times 25$ grid points, respectively for the two resolutions. The center of the model domains was at 48°N and 71°W, and the Saguenay region was always located in the central area of the two domains (Fig. 1).

The MC2 initial conditions and boundary tendencies of the 10-km resolution run were provided by a 35-km coarse resolution run of Yu et al. (1997). The results of the 10-km run were then used to drive the 5-km experiment. In mountainous regions, local weather can be affected by orographic details. If topography is not resolved adequately, a model could thus produce an erroneous simulation. Two spatial resolution topography (18 km and 900 m) datasets were used in this study. The 18-km U.S. Navy global topography dataset was used for the 10-km runs. The 900-m topography from the global Digital Elevation Model developed by the Global Land One-km Base Elevation project at the National Oceanic and Atmospheric Administration's National Geophysical Data Center was used in the 5-km runs.

For the two land surface schemes, the parameters of the force–restore method (Table 2) were initialized using CMC archived data. The initialization of CLASS parameters listed in Table 2 was done using an Environment Canada 1-km resolution GIS soil and vegetation database. The best way to initialize soil moisture is still a subject of active research. In the current study, we used CMC soil moisture index analysis to initialize the soil moisture content for both the force–restore method and CLASS. This analysis is based on the error feedback for a short forecast of dewpoint temperature at the ground using the CMC Regional Finite Element model (35-km resolution). The error in dewpoint temperature forecast is assumed to be due to incorrect soil moisture specification. A correction is then applied to the soil moisture index using the error information obtained in dewpoint temperature forecast. Precipitation is not directly assimilated in the analysis. The initialized soil moisture content in most areas of the model domain was

between saturation and field capacity, indicating wet soil conditions. In fact, 1996 had a wet and early summer with high antecedent moisture conditions. To test the effect of initial soil moisture on the simulated PR48, a dry soil moisture field (at wilting point) was also used to initialize the 5-km simulations. The comparison of the simulated domain-averaged PR48 from the ''dry'' runs with the ''normal'' (wet in this case) runs shows that the difference in PR48 was 4.1 mm or 14.7% for the force–restore method, and 1.2 mm or 4.5% for CLASS. Thus CLASS is less sensitive to the accuracy of the initial soil moisture compared to the force–restore method, for the accumulated precipitation. The CMC soil moisture index analysis was done at coarse resolution with few field observations for verification, and its potential impact on precipitation forecast could be significant. However, in our case the error introduced in the initialization of soil moisture has no significant effect on the simulated accumulated precipitation. At this stage, we have no objective method for obtaining alternative values of initial soil moisture.

4. Results and discussions

a. Precipitation

In this section, we focus mainly on the 48-h accumulated precipitation simulation using the MC2/CLASS and MC2/force–restore models. The simulated precipitation time series at different spatial resolutions will be compared with rain gauge values. We will provide both a qualitative and quantitative comparison of the model simulation results and observations. To gain further insight into how precipitation forecasts are affected by different land use types, we will report and discuss precipitation results from three more MC2/CLASS runs at 10 km under uniform coniferous tree, grass, and bare soil conditions.

Figure 2 shows a comparison of the 48-h accumulated precipitation of MC2/CLASS and MC2/force–restore at 10- and 5-km resolutions with rain gauges. Note that only the Saguenay region and its immediate vicinity, covering an area of 800×800 km^2 (Fig. 1), are shown in these figures. This region received the heaviest precipitation during the storm. Figure 2 shows the overall model-simulated PR48 patterns obtained with the two land surface schemes are qualitatively similar. The pattern shows more detailed structure at 5-km resolution (Figs. 2c and 2d) than at 10 km (Figs. 2a and 2b). Two strong precipitation centers on the windward and upslope side of the mountainous regions are successfully simulated by both land surface schemes at 10- and 5-km resolutions: one over the southern hill with PR48 $>$ 210 mm, and another over the northern hill with PR48 $>$ 240 mm. This is consistent with the observations discussed in section 3a. The effect of orography on the precipitation is thus well simulated. In comparison with rain gauge observations, MC2/CLASS (Figs. 2a and 2c) captures the precipitation features more clearly and realistically than MC2/force–restore (Figs. 2b and 2d), especially for the northern precipitation maximum. More quantitative measures of model error will be presented later. The spatial distributions of the simulated precipitation rate at 1800 UTC 20 July 1996 are compared with a snapshot of a GOES infrared image taken at 1745 UTC 20 July 1996 (Fig. 3). The GOES infrared image (Fig. 3c) shows two deep cloud clusters located in the northern central part of the model domain. The brightness temperature at cloud top is lower than -40°C, and the cloud albedo retrieved from the visible channel is over 50% (figure not shown), implying a high water content in the clouds. These deep clouds with high water content usually produce heavy precipitation (Grassotti and Garand 1994). Both land surface schemes produce two heavy precipitation centers with a precipitation rate of over 7 mm h^{-1} (Figs. 3a and 3b). Note that the brightness temperature retrieved from the GOES infrared image does not give a direct measure of the precipitation rate.

The first quantitative comparison is to compare the observed and simulated 48-h accumulated precipitation using all 46 rain gauge observations. The simulated values of PR48 from the nearest neighbor to the gauge locations were extracted from all four runs. The comparison is summarized in Table 3. The mean bias error (mbe) is an indicator of model bias and the root-mean-square (rms) error measures the model accuracy. The observed maximum 48-h accumulated precipitation (max PR48) is 274.3 mm, and the closest simulated value of 221.2 mm is given by MC2/force–restore at 5-km resolution. The best values of mbe and the rms error are -8.8 and 40.7 mm, respectively, obtained with MC2/CLASS at 5 km. Since mbe and rms error are more meaningful error measures than max PR48, we conclude that MC2/CLASS at 5 km gives the best results. Its max PR48 value is 216.1 mm, only 5.1 mm less than the best model case of MC2/force–restore at 5 km. Note also that the strongest recorded precipitation does not necessarily coincide with the real maximum of the precipitation event. For all four model runs, the southern simulated precipitation center is displaced 20–30 km farther north of the location of maximum rain gauge PR48 value (274.3 mm; Fig. 2). It is MC2/CLASS at 5 km that gives the best simulated max PR48 value (261.3 mm) for the southern precipitation center. In summary, there is a systematic improvement in the PR48 simulation for both MC2/CLASS and MC2/force–restore as the resolution is increased as measured by the mbe and rms error. At the same resolution, MC2/CLASS gives smaller mbe and rms errors than MC2/force–restore.

We next examine the timing of the observed and simulated precipitation. Comparison of six simulated precipitation time series at different spatial resolutions with rain gauges is shown in Fig. 4. The simulated precipitation values from the nearest neighbor to the rain gauge locations were extracted for all four runs. Figures 4a

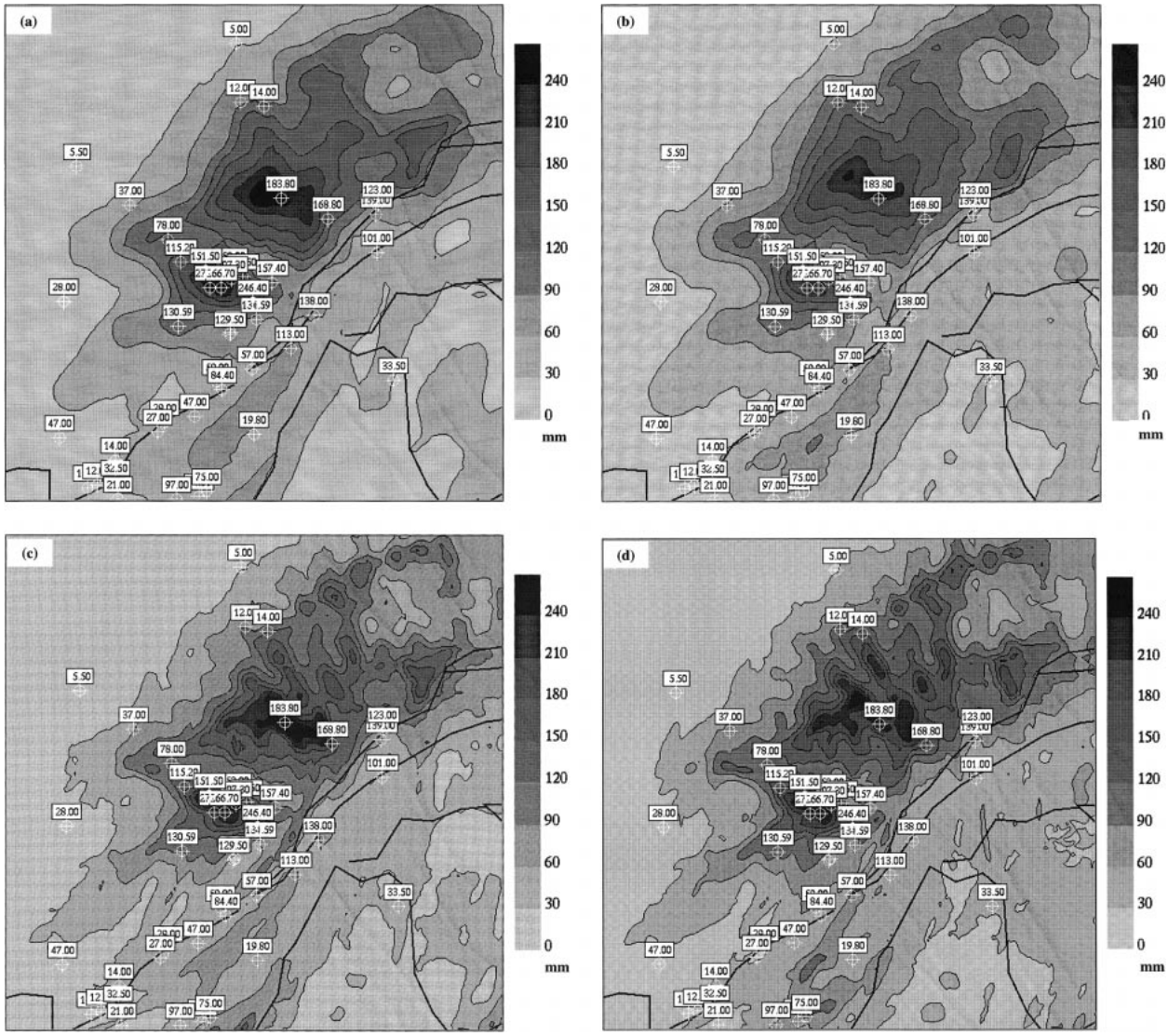

FIG. 2. Comparison of observed and simulated 48-h accumulated precipitation for the Saguenay region and its immediate vicinity for different resolutions: (a) MC2/CLASS at 10 km, (b) MC2/force–restore at 10 km, (c) MC2/CLASS at 5 km, and (d) MC2/force–restore at 5 km. The value inside the rectangular boxes shows meteorological station observations of the 48-h accumulated precipitation, with the cross symbol marking the station location. Contours of the simulated 48-h accumulated precipitation are shown using intervals of 30 mm.

and 4b show the precipitation time series corresponding to gauges that recorded the two largest values of PR48 (274.3 and 266.7 mm), and the model results. The remaining panels of Fig. 4 show gauges with values of PR48 ranging from 134.6 to 207.3 mm. In general, a satisfactory forecast is obtained. The simulated and gauge time series are similar in shape except for Fig. 4d, where the observed sharp increase late in the time series was only captured by MC2/CLASS. In comparison with observations, MC2/CLASS at 5 km gives the best results, with MC2/CLASS at 10 km being comparable to MC2/force–restore at 5 km. A common problem for all simulations is the initial slow rate of precipitation increase. This is due to the spinup period in the simulations. Since MC2 is initiated with no clouds due to the lack of such information in the CMC analysis, a possible solution is to use a physical initialization as proposed by Krishnamurti et al. (1997), but it is beyond the scope of this study.

Figure 5 shows a point-by-point scatterplot of the simulated 48-h accumulated precipitation for all four runs versus observations from the 46 rain gauges. Regression lines from a least squares fit are also provided in Fig. 5. The slopes of all four regression lines are less than unity, and it is MC2/CLASS at 5 km that gives the best result. We have already seen that the PR48 values are generally underestimated in all four runs, resulting in the negative mbe values in Table 3. The underestimation occurs for accumulated precipitation larger than 50–60 mm, as shown in Fig. 5. For smaller accumulated

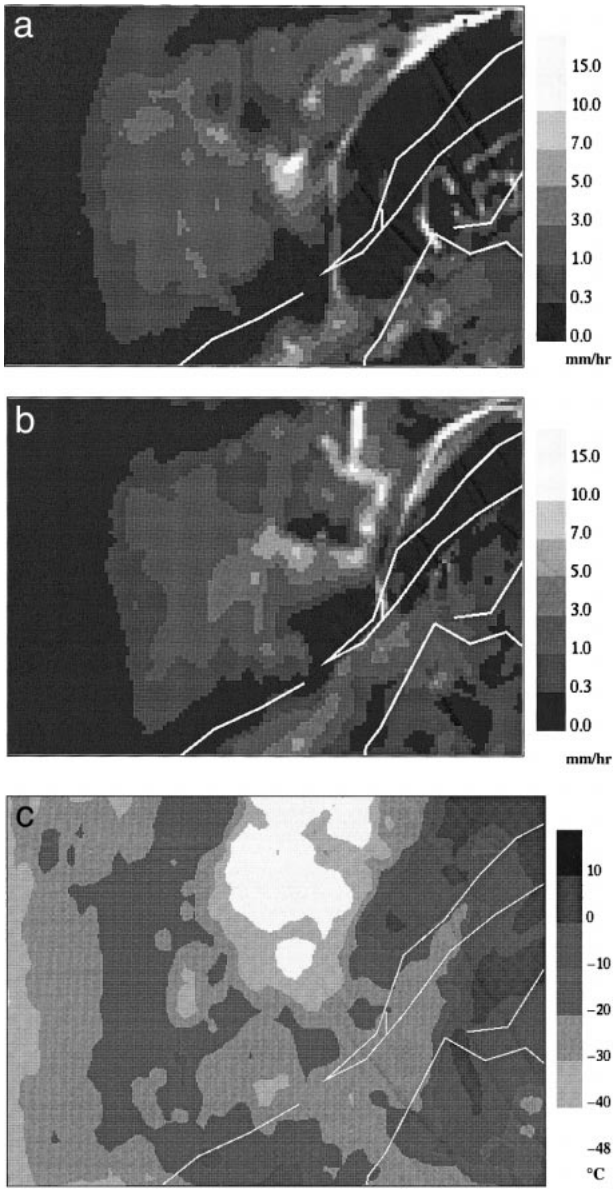

FIG. 3. (a) The 5-km MC2/CLASS simulated precipitation rate at 1800 UTC 20 Jul 1996. (b) The 5-km MC2/force–restore simulated precipitation rate at 1800 UTC 20 Jul 1996. (c) Brightness temperature (°C) from infrared channel (11 μm) of *GOES-8*. The image was taken at 1745 UTC 20 Jul 1996. The bright area represents temperatures colder than −40°C, indicative of deep cloud clusters.

precipitation, the simulated PR48 values are generally larger than observed. Two important conclusions can be drawn from Table 3 and Fig. 5. The first is that MC2/force–restore benefits more from increasing spatial resolution than MC2/CLASS in model accuracy, as seen from the mbe and rms error values in Table 3. The improvement of mbe and rms error values are, respectively, from −16.00 to −10.00 mm, and 46.9 to 43.9 mm, as the resolution is increased from 10 to 5 km, for MC2/force–restore. While for MC2/CLASS, the mbe

TABLE 3. Statistics of the comparison of the simulated 48-h accumulated precipitation with rain gauge observations. Max PR48, mbe and rms error indicate, respectively, the maximum, mean bias error, and root-mean-square error. The best results are italic. The maximum simulated precipitation is taken at the same grid box of the observed maximum for the four model cases.

	Max PR48 (mm)	Mbe (mm)	Rms error (mm)
Observation	274.3	—	—
MC2/CLASS 5 km	216.1	*−8.8*	*40.7*
MC2/CLASS 10 km	218.4	−10.8	42.7
MC2/force–restore 5 km	*221.2*	−10.0	43.9
MC2/force–restore 10 km	200.9	−16.0	46.9

and rms error improvements are marginal, from −10.8 to −8.8 mm, and 42.7 to 40.7 mm, respectively. The second conclusion is that the model accuracy of MC2/CLASS at 10 km is comparable to that of MC2/force–restore at 5 km. In fact, these two points are related.

We now examine in detail the reason for the second conclusion. CLASS represents land surface vegetation characteristics in a more sophisticated manner than the force–restore method, as reviewed in section 2. In this case, each CLASS grid square is divided into two separate subareas: bare soil and vegetation cover. Vegetation is further divided into two major types: coniferous and deciduous trees. This thus accounts for the variations of the surface vegetation characteristics within a grid box. This subgrid-scale information is used by CLASS, and the CLASS-computed variables that are fed back to MC2 on a 10×10 km^2 grid are thus equivalent to a higher effective resolution than 10 km. This higher effective resolution for surface characteristics is not found in the force–restore method.

Figure 6 shows a point-by-point scatterplot of the simulated 48-h accumulated precipitation for five 10-km runs (MC2/CLASS with actual vegetation conditions, uniform coniferous trees, grass, bare soil, and MC2/force–restore) versus observations from the 46 rain gauges. Regression lines from a least squares fit are also provided in Fig. 6. The comparison results are summarized in Table 4. An important conclusion is that the differences in accumulated precipitation between MC2/CLASS with actual vegetation conditions and coniferous tree conditions are small. This is because for actual vegetation conditions, we use mixed forest (coniferous and deciduous trees) and coniferous forest vegetation in the Saguenay region and its immediate vicinity. While for coniferous tree conditions, only coniferous forest is used for the same region. Differences in the parameter values of coniferous and deciduous trees are not significant for summertime, and the soil was saturated as well. The simulated accumulated precipitation was thus similar. The differences between bare soil condition and force–restore are also small (Table 4, Fig. 6). This is because there is no physically based vegetation module in the force–restore method.

Since the differences in results between actual veg-

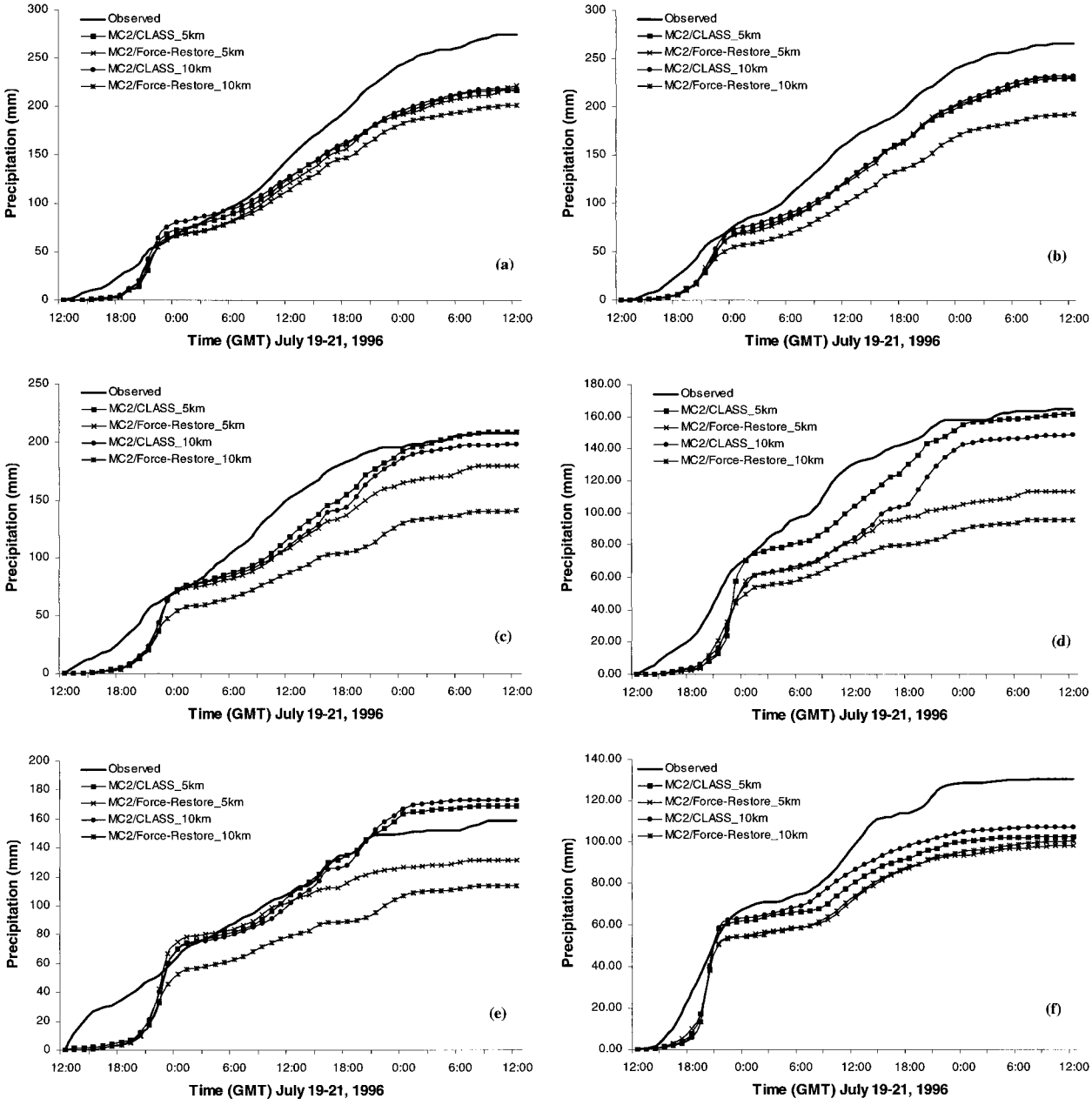

FIG. 4. Comparison of simulated precipitation time series of MC2/CLASS and MC2/force–restore at 10- and 5-km resolutions with observations, at rain gauge number (a) 061020, (b) 061022, (c) 061001, (d) 7060400, (e) 7063690, and (f) 04750.

etation conditions and coniferous tree conditions are insignificant, we cannot conclude the subgrid vegetation division used by CLASS is the only (or major) factor accountable for the improvement of the precipitation simulation. However, it is interesting that the regression line obtained with grass conditions falls between the regression lines with actual vegetation and bare soil conditions. This is because the differences in the parameter values among the three land types of coniferous and deciduous trees, grass, and bare soil are large, and the soil was saturated. Another factor is that precipitation is only the end product of the MC2/CLASS coupled model. In other words, different vegetation cover types affect directly sensible and latent heat fluxes. These fluxes in turn influence the cloud formation and, hence, the precipitation. Thus the sensitivity of precipitation to the use of vegetation cover types is lower compared to that of sensible and latent heat fluxes. At the same time, we note the Saguenay case used in this experiment may not be a significant case to show the power of CLASS sub-

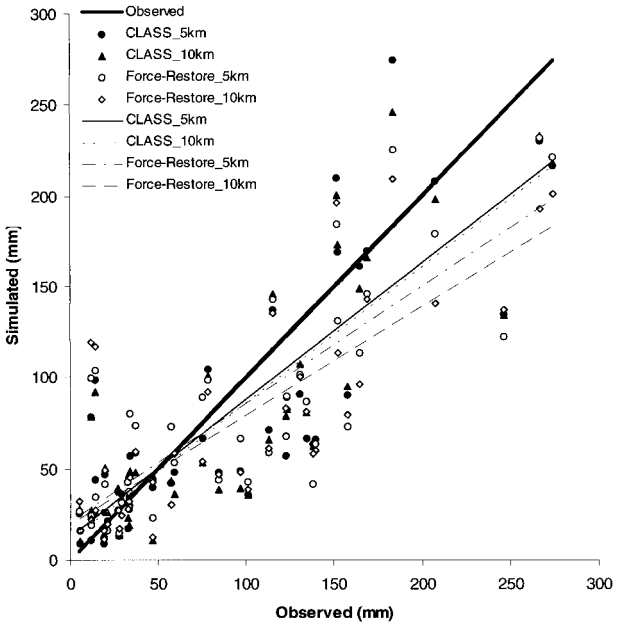

FIG. 5. Scatterplot of 48-h accumulated precipitation (in mm) from MC2/CLASS and MC/force–restore at 10- and 5-km resolutions vs observations from 46 rain gauges. Regression lines from a least squares fit are also provided.

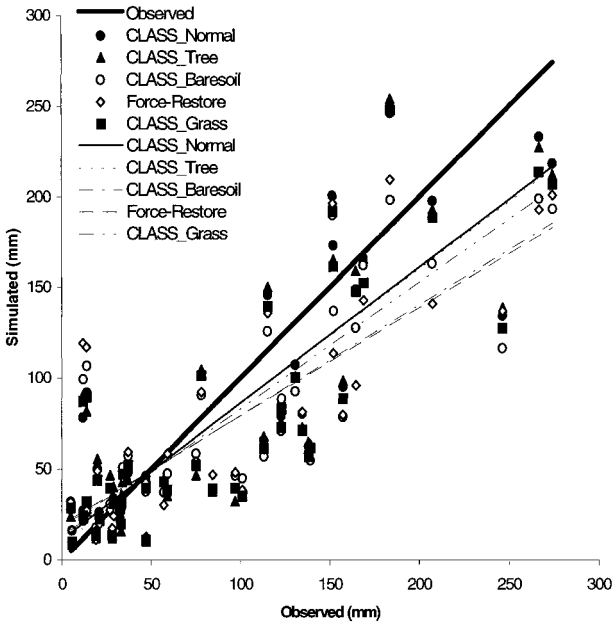

FIG. 6. Scatterplot of 48-h accumulated precipitation (in mm) for five 10-km runs (MC2/CLASS with actual vegetation conditions, uniform coniferous trees, grass, and bare soil, and MC2/force–restore) vs observations from the 46 rain gauges. Regression lines from a least squares fit are also provided.

grid vegetation division type, as trees are the dominant vegetation in the Saguenay region. Therefore, more cases are needed for further study.

b. Domain-averaged precipitation, and sensible and latent heat fluxes

The difference in the 48-h accumulated precipitation simulations of MC2/CLASS and MC2/force–restore is clearly due to the use of different land surface schemes. To gain further insight into the mechanisms responsible for this, we now examine the simulated domain-averaged precipitation, and sensible and latent heat fluxes for all four runs. The domain of interest is again the Saguenay region and its immediate vicinity (Fig. 1). The domain-averaged accumulated precipitation, and latent heat and sensible heat flux time series computed by MC2/CLASS and MC2/force–restore at 5 km are shown in Fig. 7. We have examined these results at 10-km resolution and found them to be similar to the 5-km results. The 10-km results are thus not shown.

The simulated domain-averaged 48-h accumulated precipitation at 5-km resolution is 54.7 mm for MC2/CLASS and 56.3 mm for MC2/force–restore, and the differences in the two time series are small (Fig. 7a). Although MC2/force–restore gives slightly more precipitation than MC2/CLASS, the difference in the domain-averaged PR48 is only 1.6 mm, less than 3%. The comparison of the domain-averaged latent and sensible heat flux time series (Fig. 7b) indicates the force–restore method produces more latent heat flux than CLASS for the entire run, while the diurnal variation of the sensible heat flux simulated by CLASS is generally larger than that by the force–restore method. We have examined the simulated incoming shortwave radiation arriving at the ground for both CLASS and the force–restore method; there is little difference between them. The sums of the simulated sensible and latent heat fluxes from MC2/CLASS and MC2/force–restore are similar, with the difference being less than 15%. The difference is thus in the partitioning of the fluxes. The force–restore method gives more evaporation, while CLASS releases more sensible heat to the atmosphere. The simulated domain-averaged 48-h accumulated evapotranspiration is 9 mm for CLASS and 11.8 mm for force–restore. It should be pointed out that the simulated latent heat flux remains significantly positive during the night, exceeding 100 W m^{-2} for many hours, while the simulated sensible heat values are quite strongly negative at night, ap-

TABLE 4. Statistics of the comparison of the simulated 48-h accumulated precipitation at 10-km resolution with rain gauge observations.

	Max PR48 (mm)	Mbe (mm)	Rms error (mm)
Observation	274.3	—	—
MC2/CLASS_normal	218.4	−10.8	42.7
MC2/CLASS_tree	212.2	−12.0	42.9
MC2/CLASS_grass	206.8	−13.5	43.7
MC2/CLASS_baresoil	193.4	−16.0	45.2
MC2/force–restore	200.9	−16.0	46.9

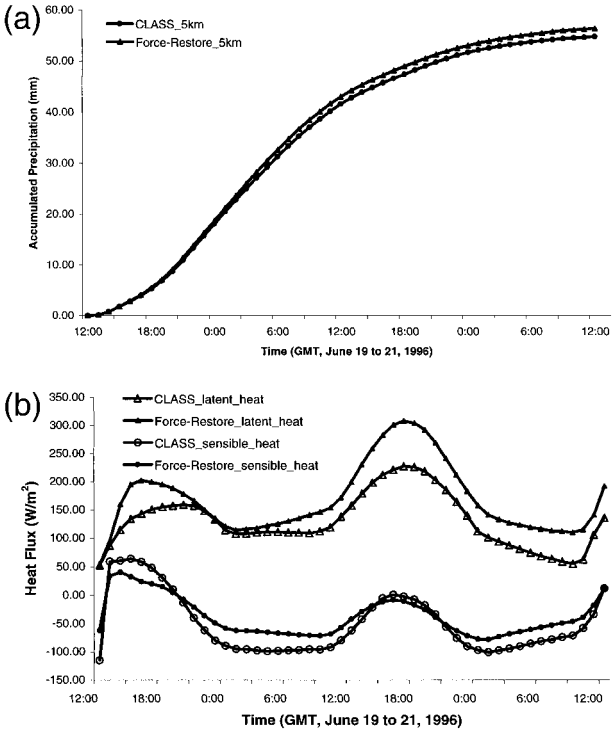

FIG. 7. (a) The domain-averaged accumulated precipitation time series computed by MC2/CLASS and MC2/force–restore at 5 km. (b) The domain-averaged latent heat and sensible heat fluxes time series computed by MC2/CLASS and MC2/force–restore at 5 km.

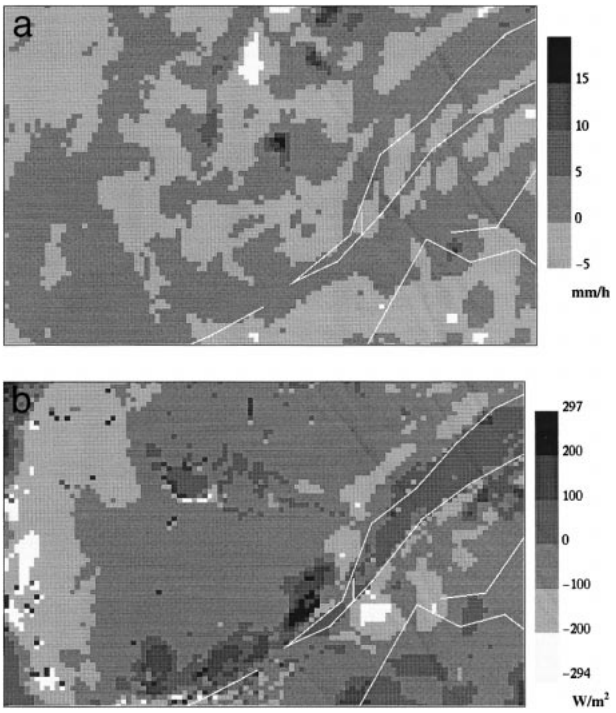

FIG. 8. (a) The differences in precipitation rate of MC2/CLASS and MC2/force–restore at 5 km taken at 1800 UTC 20 Jul 1996. (b) The differences in sensible heat flux of MC2/CLASS and MC2/force–restore at 5 km taken at 1800 UTC 20 Jul 1996.

proaching 100 W m^{-2}. These values seem to be extreme. The equations used in CLASS and the force–restore method for evapotranspiration and sensible heat flux calculations are widely used in many other land surface schemes. The extreme values of the simulated sensible and latent heat fluxes may be due to the severe precipitation case, but further investigation into this aspect is needed.

The higher evaporation in force–restore compared to CLASS results in more cooling, as the sums of the simulated sensible and latent heat fluxes are similar in the two cases. This affects the sensible heat flux at the ground, and the vertical movement of water vapor, which in turn can result in a different precipitation distribution. After the first hour of model integration, the sensible heat flux simulated by MC2/CLASS has a different distribution compared with that of MC2/force–restore. Higher values of sensible heat flux produced by MC2/CLASS are usually found along the valley of the St. Lawrence River. Figure 8 shows the differences in precipitation rate and sensible heat flux between MC2/CLASS and MC2/force–restore at 1800 UTC 20 July 1996. This time instant coincides with the occurrence of the second wave of heavy precipitation. The differences in sensible heat flux are substantial, but are not found at the same locations as the differences in precipitation rate. The area of higher precipitation rate is generally downstream of the region of higher sensible heat flux. A similar result has been reported by Beljaars et al. (1996), using the European Centre for Medium-Range Weather Forecasts model in their short- and medium-range precipitation forecast study. Our case study shows that the surface heat fluxes can significantly affect the precipitation distribution, even for a short-range precipitation forecast. The end result is that the use of an advanced land surface scheme such as CLASS can help to improve the positioning of the simulated precipitation (Table 3, Fig. 5).

5. Conclusions

We have used the severe precipitation case of 19–21 July 1996 in the Saguenay region of Québec, Canada, to explore the role of land surface schemes for short-range, high spatial resolution precipitation simulations. The heavy precipitation led to flooding in this area. A series of 48-h simulations with spatial resolutions of 10 and 5 km were performed using the MC2/CLASS and the MC2/force–restore modeling systems. We compared the simulated precipitation with observations, both qualitatively and quantitatively. An analysis of the sensitivity of domain-averaged precipitation, and sensible and latent heat fluxes to the use of CLASS and the force–restore method at 5-km resolution was carried out, in order to gain further insight into the mechanisms responsible for the differences in the results obtained. The following conclusions can be drawn from this study.

- The comparison of the 48-h accumulated precipitation with rain gauges indicates that MC2/CLASS at 5-km resolution gave the best results.
- The model accuracy of MC2/CLASS at 10-km resolution is comparable to that of MC2/force–restore at 5 km. The main reason is that CLASS can better represent the variations of the grid surface vegetation characteristics.
- The total simulated domain-averaged precipitation, and the sum of sensible and latent heat fluxes from MC2/CLASS and MC2/force–restore are similar. The major difference is in the partitioning of the simulated sensible and latent heat fluxes.
- The result shows that the positioning of the simulated precipitation is improved by using CLASS over the force–restore method, as revealed by the rms error analysis and the scatterplot of simulated and observed values.

Finally, the overall results suggest that the impact of land surface schemes can be significant in short-range, high spatial resolution precipitation simulations, especially in regions with complicated vegetation variations.

Acknowledgments. This research project is partially supported by the Network for Computing and Mathematical Modeling, a multiuniversity initiative founded by the Natural Science and Engineering Research Council (NSERC) of Canada. The project is also supported by a NSERC Strategic Project award (Simulation of Severe Precipitation and Flash Floods).

REFERENCES

Avissar, R., and R. A. Pielke, 1989: A parameterization of heterogeneous land surface for atmospheric numerical models and its impact on regional meteorology. *Mon. Wea. Rev.,* **117,** 2113–2136.

Beljaars, A. C. M., P. Viterbo, M. J. Miller, and A. K. Betts, 1996: The anomalous rainfall over the United States during July 1993: Sensitivity to land surface parameterization and soil moisture anomalies. *Mon. Wea. Rev.,* **124,** 362–383.

Benoit, R., M. Desgagné, P. Pellerin, S. Pellerin, Y. Chartier, and S. Desjardins, 1997: A semi-Lagrangian, semi-implicit wide-band atmospheric model suited for finescale process studies and simulation. *Mon. Wea. Rev.,* **125,** 2382–2415.

Bouttier, F., J.-F. Mahfouf, and J. Noilhan, 1993: Sequential assimilation of soil moisture from atmospheric low-level parameters. Part II: Implementation in a mesoscale model. *J. Appl. Meteor.*, **32,** 1352–1364.

Chen, T. H., and Coauthors, 1997: Cabauw experimental results from the Project for Intercomparison of Land-Surface Parameterization Schemes. *J. Climate,* **10,** 1194–1215.

Clapp, R. B., and G. M. Hornberger, 1978: Empirical equations for some soil hydraulic properties. *Water Resour. Res.,* **14,** 601–604.

Deardorff, J. W., 1978: Efficient prediction of ground surface temperature and moisture, with inclusion of a layer of vegetation. *J. Geophys. Res.,* **83** (C4), 1889–1903.

Delage, Y., and D. Verseghy, 1995: Testing the effects of a new land surface scheme and of initial soil moisture conditions in the Canadian Global Forecast Model. *Mon. Wea. Rev.,* **123,** 3305–3317.

——, L. Wen, and J.-M. Bélanger, 1999: Aggregation of parameters for the land surface model CLASS. *Atmos.–Ocean,* **37,** 157–178.

Ducoudré, N. I., K. Laval, and A. Perrier, 1993: SECHIBA, a new set of parameterizations of the hydrologic exchanges at the land–atmosphere interface within the LMD atmospheric general circulation model. *J. Climate,* **6,** 248–273.

Gal-Chen, T., and R. C. J. Sommerville, 1975: On the use of a coordinate transformation for the solution of the Navier–Stokes equations. *J. Comput. Phys.,* **17,** 209–228.

Garratt, J. R., 1993: Sensitivity of climate simulations to land-surface and atmospheric boundary-layer treatments—A review. *J. Climate,* **6,** 419–449.

Grassotti, C., and L. Garand, 1994: Classification-based rainfall estimation using satellite data and numerical forecast model fields. *J. Appl. Meteor.,* **33,** 159–178.

Henderson-Sellers, A., Z. L. Yang, and R. E. Dickinson, 1993: The Project for Intercomparison of Land-Surface Parameterization Schemes. *Bull. Amer. Meteor. Soc.,* **74,** 1335–1349.

Koster, R. D., and M. Suarez, 1992: Modeling the land surface boundary in climate models as a composite of independent vegetation stands. *J. Geophys. Res.,* **97,** 2697–2715.

Krishnamurti, T. N., H. S. Bedi, G. D. Rohaly, D. K. Oosterhof, R. C. Torres, and E. Williford, 1997: Physical initialization. *Numerical Methods in Atmospheric and Oceanic Modelling,* C. A. Lin, R. Laprise, and H. Ritchie, Eds., NRC Research Press, 369–398.

Kuo, H. L., 1974: Further studies on the parameterization of the influence of cumulus convection on large-scale flow. *J. Atmos. Sci.,* **31,** 1232–1240.

Mailhot, J., R. Sarrazin, B. Bilodeau, N. Brunet, and G. Pellerin, 1997: Development of the 35-km version of the Canadian regional forecast system. *Atmos.–Ocean,* **35,** 1–28.

Manabe, S., 1969: Climate and the ocean circulation: The atmospheric circulation and the hydrology of the earth's surface. *Mon. Wea. Rev.,* **97,** 739–805.

Milly, P. C. D., and K. A. Dunne, 1994: Sensitivity of the global water cycle to the water-holding capacity of land. *J. Climate,* **7,** 506–526.

Mintz, Y., 1984: The sensitivity of numerically simulated climates to land-surface boundary conditions. *The Global Climate,* J. Houghton, Ed., Cambridge University Press, 79–105.

Nobre, C. A., P. J. Sellers, and J. Shukla, 1991: Amazonian deforestation and regional climate change. *J. Climate,* **4,** 957–988.

Noilhan, J., and S. Planton, 1989: A simple parameterization of land surface processes for meteorological models. *Mon. Wea. Rev.,* **117,** 536–549.

——, and P. Lacarrère, 1995: GCM grid-scale evaporation from mesoscale modeling. *J. Climate,* **8,** 206–223.

Oglesby, R. J., 1991: Springtime soil moisture variability, and North American drought as simulated by the NCAR Community Climate Model I. *J. Climate,* **4,** 890–897.

Rosenzeig, C., and F. Abramopoulos, 1997: Land-surface model development for the GISS GCM. *J. Climate,* **10,** 2040–2054.

Rowntree, P. R., and J. A. Bolton, 1983: Simulation of the atmospheric response to soil moisture anomalies over Europe. *Quart. J. Roy. Meteor. Soc.,* **109,** 501–526.

Sellers, P. J., Y. Mintz, Y. C. Sud, and A. Dalcher, 1986: A simple biosphere model (SiB) for use within general circulation models. *J. Atmos. Sci.,* **43,** 505–531.

——, D. A. Randall, C. J. Collatz, J. A. Berry, C. B. Field, D. A. Dazlich, C. Zhang, and G. C. Collelo, 1996: A revised land surface parameterization (SiB) for atmospheric GCMs. Part I: Model formulation. *J. Climate,* **9,** 676–705.

Shao, Y. P., and A. Henderson-Sellers, 1996: Modelling soil moisture: A Project for Intercomparison of Land Surface Parameterization Schemes Phase 2(b). *J. Geophys. Res.,* **101,** 7227–7250.

Sundqvist, H., 1978: A parameterization scheme for non-convective condensation including prediction of cloud water content. *Quart. J. Roy. Meteor. Soc.,* **104,** 677–690.

Tanguay, M., A. Robert, and R. Laprise, 1990: A semi-implicit semi-

Lagrangian fully compressible regional forecast model. *Mon. Wea. Rev.,* **118,** 1970–1980.

Thomas, S. J., C. Girard, R. Benoit, M. Desgagné, and P. Pellerin, 1998: A new adiabatic kernel for the MC2 model. *Atmos.–Ocean,* **36,** 241–270.

Verseghy, D. L., 1991: CLASS—A Canadian land surface scheme for GCMS. I. Soil model. *Int. J. Climatol.,* **11,** 111–133.

——, N. A. McFarlane, and M. Lazare, 1993: CLASS—A Canadian land surface scheme for GCMS. II. Vegetation model and coupled runs. *Int. J. Climatol.,* **13,** 347–370.

Wen, L., J. Gallichand, A. A. Viau, Y. Delage, and R. Benoit, 1998: Calibration of the CLASS model and its improvement under agricultural conditions. *Trans. ASAE,* **41,** 1345–1351.

Wood, E. F., D. P. Lettenmaier, and V. Zartarian, 1992: A land surface hydrology parameterization with sub-grid variability for general circulation models. *J. Geophys. Res.,* **97** (D3), 2717–2728.

Yang, Z.-L., and R. E. Dickinson, 1996: Description of the Biosphere–Atmosphere Transfer Scheme (BATS) for the soil moisture workshop and evaluation of its performance. *Global Planet. Change,* **13,** 117–134.

——, ——, A. Henderson-Sellers, and A. J. Pitman, 1995: Preliminary study of spin-up processes in land surface models with the first stage data of Project for Intercomparison of Land Surface Parameterization Schemes Phase 1(a). *J. Geophys. Res.,* **100** (D8), 16 553–16 578.

Yu, W., C. Lin, and R. Benoit, 1997: High resolution simulation of the severe precipitation over Saguenay, Québec region in July 1996. *Geophys. Res. Lett.,* **24,** 1952–1954.

——, ——, ——, and I. Zawadzki, 1998: High resolution model simulation of precipitation and evaluation with Doppler radar observation. *Water. Sci. Technol.,* **37,** 179–186.